ORIGINAL RESEARCH

Synthesis of silver nanoparticles using *Dioscorea bulbifera* tuber extract and evaluation of its synergistic potential in combination with antimicrobial agents

Sougata Ghosh[1]
Sumersing Patil[1]
Mehul Ahire[1]
Rohini Kitture[2]
Sangeeta Kale[3]
Karishma Pardesi[4]
Swaranjit S Cameotra[5]
Jayesh Bellare[6]
Dilip D Dhavale[7]
Amit Jabgunde[7]
Balu A Chopade[1]

[1]Institute of Bioinformatics and Biotechnology, University of Pune, Pune, [2]Department of Electronic Science, Fergusson College, Pune, [3]Department of Applied Physics, Defense Institute of Advanced Technology, Girinagar, Pune, [4]Department of Microbiology, University of Pune, Pune, [5]Institute of Microbial Technology, Chandigarh, [6]Department of Chemical Engineering, Indian Institute of Technology, Mumbai, [7]Garware Research Centre, Department of Chemistry, University of Pune, Pune, India

Background: Development of an environmentally benign process for the synthesis of silver nanomaterials is an important aspect of current nanotechnology research. Among the 600 species of the genus Dioscorea, *Dioscorea bulbifera* has profound therapeutic applications due to its unique phytochemistry. In this paper, we report on the rapid synthesis of silver nanoparticles by reduction of aqueous Ag^+ ions using *D. bulbifera* tuber extract.

Methods and results: Phytochemical analysis revealed that *D. bulbifera* tuber extract is rich in flavonoid, phenolics, reducing sugars, starch, diosgenin, ascorbic acid, and citric acid. The biosynthesis process was quite fast, and silver nanoparticles were formed within 5 hours. Ultraviolet-visible absorption spectroscopy, transmission electron microscopy, high-resolution transmission electron microscopy, energy dispersive spectroscopy, and x-ray diffraction confirmed reduction of the Ag^+ ions. Varied morphology of the bioreduced silver nanoparticles included spheres, triangles, and hexagons. Optimization studies revealed that the maximum rate of synthesis could be achieved with 0.7 mM $AgNO_3$ solution at 50°C in 5 hours. The resulting silver nanoparticles were found to possess potent antibacterial activity against both Gram-negative and Gram-positive bacteria. Beta-lactam (piperacillin) and macrolide (erythromycin) antibiotics showed a 3.6-fold and 3-fold increase, respectively, in combination with silver nanoparticles selectively against multidrug-resistant *Acinetobacter baumannii.* Notable synergy was seen between silver nanoparticles and chloramphenicol or vancomycin against *Pseudomonas aeruginosa*, and was supported by a 4.9-fold and 4.2-fold increase in zone diameter, respectively. Similarly, we found a maximum 11.8-fold increase in zone diameter of streptomycin when combined with silver nanoparticles against *E. coli*, providing strong evidence for the synergistic action of a combination of antibiotics and silver nanoparticles.

Conclusion: This is the first report on the synthesis of silver nanoparticles using *D. bulbifera* tuber extract followed by an estimation of its synergistic potential for enhancement of the antibacterial activity of broad spectrum antimicrobial agents.

Keywords: *Dioscorea bulbifera* tuber extract, silver nanoparticles, antimicrobial synergy

Introduction

Nanoparticles have received considerable attention in recent years due to their wide range of applications in the fields of catalysis, photonics, optoelectronics, biological tagging, pharmaceutical applications environmental pollution control, drug delivery systems, and material chemistry.[1–3] Although there has been extensive research on the chemical synthesis of nanoparticles, these particles have several potential hazards, including carcinogenicity, genotoxicity, cytotoxicity, and general toxicity.[4,5] There is a

Correspondence: Balu A Chopade
Institute of Bioinformatics and Biotechnology, University of Pune, Pune 411007, India
Tel +91 20 2569 0442
Fax +91 20 2569 0087
Email directoribb@.unipune.ac.in

483

need to develop clean, nontoxic, and ecofriendly procedures for synthesis and assembly of nanoparticles.[4] Synthesis of metal nanoparticles is solely dependent on knowledge of micro-organisms and their behavior, which play a crucial role. Against this background, researchers have been working extensively on extracellular and intracellular synthesis of metal nanoparticles using bacteria, fungi, yeasts, and many other biological sources.[6–8] One of the major drawbacks to using microbes for bioreduction is the need to maintain aseptic conditions, which is not only labor-intensive but also very expensive in terms of industrial production costs. There are reports on the synthesis of nanoparticles using lemon grass and neem leaves.[9,10] Leaf extracts have been used for synthesis of silver nanoparticles, which has highlighted the possibility of rapid synthesis and may also reduce the steps involved in downstream processing, thereby making the process more economical and cost-efficient.[11–13] Sastry et al, Shankar et al, and Ankamwar et al have worked extensively on the biosynthesis of metal nanoparticles from various plant sources.[6,11,14] They have reported on synthesis of nanoparticles having exotic shapes and morphologies.[9] The spectacular success in this field has opened up the prospect of developing "green synthesis" methods for metal nanoparticles with tailor-made structural properties using benign starting materials. Silver has been used as a healing and antibacterial agent throughout the world for thousands of years.[15] Its benefit over the use of antibiotics can be used as a powerful strategy to combat the increasing spread of multidrug resistance resulting from broad use of antibiotics. Therefore, the clinical efficacy of antibiotics has been compromised. Antibiotic resistance has become a serious problem threatening the health of human beings.[16–20] Of all the inorganic antimicrobial agents, silver elements and nanoparticle compounds have been the most extensively tested. Sondi and Salopek-Sondi recently demonstrated that silver (0) nanoparticles are quite effective antimicrobial agents against *Escherichia coli*.[21] In addition, silver nanoparticles have excellent properties in terms of conformational entropy in polyvalent binding, which makes it easy for them to attach to flexible polymeric chains of antibiotics.[22,23] Moreover, silver nanoparticles have well developed surface chemistry and chemical stability, and are of appropriate size. They are able to maintain a constant shape and size in solution. Thus, silver nanoparticles are a good choice as inorganic nanomaterials in combination with various classes of antibiotics for use against pathogenic micro-organisms.

Dioscorea bulbifera is unique among 600 species of the genus Dioscorea due to its species-specific phytochemistry,

supporting its widespread application in therapeutics.[24] *D. bulbifera* tuber extract is rich in polyphenolic compounds, especially flavonoids and catechin, which have contributed to its pronounced antioxidant and antidiabetic properties.[25–27] In an earlier report, we reported synthesis of gold nanoparticles using *D. bulbifera*.[28] However, to date, there are no reports on the synthesis of silver nanoparticles using *D. bulbifera* tuber extract. In view of this background, a detailed investigation is required into its potential for use in the synthesis of silver nanoparticles, along with characterization and application in therapeutics. Similarly, there are no reports including thorough evaluation of the role of silver nanoparticles in the enhancement of efficacy of a diverse group of antibiotics, ie, β-lactams, cephalosporins, aminoglycosides, rifamycins, glycopeptides, quinolones, tetracyclines, trimethoprim, carbapenems, cyclic peptides, and macrolides, against a wide group of Gram-positive and Gram-negative bacteria.

In this paper, we report for the first time the synthesis of silver nanoparticles by reduction of aqueous Ag^+ ions with the assistance of *D. bulbifera* tuber extract. We have used tuber broth for the biogenic reduction of Ag^+ ions. Our objective in this work was to reduce ionic silver to nanoparticles using a biomaterial that addresses two major factors, ie, the need for the biomaterial to be environmentally benign and produce no toxic industrial waste and for it to be cost-effective and easily produced. We also investigated the effects of reaction conditions, such as temperature and $AgNO_3$ concentration, on the rate of synthesis of silver nanoparticles. We studied their antimicrobial effects at various concentrations against a wide range of Gram-negative and Gram-positive bacteria. Furthermore, we evaluated the silver nanoparticles in combination with various groups of antibiotics for synergistic enhancement of antimicrobial activity against pathogenic bacteria. Herein, we present the first detailed study of the synergistic potential of biogenic silver nanoparticles in combination with 22 different antibiotics against 14 potent bacterial pathogens.

Materials and methods
Plant material and preparation of extract
D. bulbifera tubers were collected from the Western Ghats region in Maharashtra, India, chopped into thin slices, and dried for two days at room temperature. The tuber extract was prepared by putting 5 g of thoroughly washed and finely ground tuber powder into a 300 mL Erlenmeyer flask with 100 mL of sterile distilled water, boiling the mixture for 5 minutes, then decanting it. The extract obtained was filtered through Whatman No 1 filter

paper. The filtrate was collected and stored at 4°C for further use.

Phytochemical analysis
Total flavonoid content
A 0.5 mL sample of *D. bulbifera* tuber extract was mixed with 0.5 mL of 2% $AlCl_3$ in methanol and incubated for 10 minutes at room temperature. After exactly 10 minutes, absorbance was recorded at 368 nm. The total phenolic content was quantified from a standard quercetin curve.[29]

Total phenolic content
A 0.125 mL sample of *D. bulbifera* tuber extract was mixed with 0.5 mL of deionized water. Folin-Ciocalteu reagent 0.125 mL was added and incubated for 5 minutes at room temperature followed by addition of 1.25 mL of 7% Na_2CO_3 solution. The volume was made up to 3 mL with distilled water followed by incubation for 90 minutes at room temperature. Absorbance was recorded at 760 nm. Total flavonoid content was estimated from a standard gallic acid curve.[30]

Starch content
Five grams of dry *D. bulbifera* tuber powder was repeatedly washed using 70% ethanol to remove sugars until the washings did not show color with an anthrone reagent. The residue was dried and boiled in 100 mL of distilled water to obtain *D. bulbifera* tuber extract without any sugars. A 1 mL sample of *D. bulbifera* tuber extract was evaporated to dryness and reconstituted in 60% perchloric acid. Thereafter, 4 mL of anthrone reagent was added, followed by boiling in a water bath for 8 minutes. The intensity of the dark green color was recorded at 630 nm, and the starch content was estimated by comparison with a standard glucose curve.[31]

Total reducing sugar
A 100 mL quantity of *D. bulbifera* tuber extract was made up to a volume of 1 mL using distilled water, and 1 mL of dinitrosalicylic reagent was added. The mixture was kept at 100°C for 5 minutes, and absorbance was recorded at 540 nm. Total reducing sugar was quantified from a standard maltose curve.[32]

Diosgenin content
A 1 mL sample of *D. bulbifera* tuber extract was evaporated to dryness, and 5 mL of 60% perchloric acid was added to the dry residue and mixed thoroughly. Absorbance was recorded at 410 nm after 10 minutes, and the diosgenin content was determined from a standard diosgenin curve.[33]

Ascorbic acid content
A 2 mL sample of *D. bulbifera* tuber extract was evaporated to dryness, followed by reconstitution in oxalic acid 4%. The sample was then brominated and 1 mL of dinitrophenyl hydrazine reagent was added, followed by two drops of 10% thiourea. After mixing thoroughly, the tube was kept at 37°C for 3 hours. The orange-red osazone crystals formed were dissolved in 7 mL of 80% sulfuric acid. Absorbance was measured at 540 nm. The content of ascorbic acid in the *D. bulbifera* tuber extract was quantified by comparison with a standard curve for ascorbic acid.[34]

Citric acid content
A 1 mL quantity of *D. bulbifera* tuber extract was evaporated to dryness and reconstituted in 1 mL of 5% trichloroacetic acid. The tube was stoppered after dropwise addition of 8 mL of anhydrous acetic anhydride, followed by incubation at 60°C for 10 minutes in a water bath. Thereafter, 1 mL of pyridine was added to each tube and restoppered, after which the tube was incubated at 60°C for 40 minutes. At the end of this period, the tube was transferred to an iced water bath for 5 minutes and absorbance was recorded at 420 nm. The total citric acid content was determined from a standard citric acid curve in the range of 10–400 µg/mL.[35]

Synthesis of silver nanoparticles
Ag^+ ions were reduced by addition of 5 mL of *D. bulbifera* tuber extract to 95 mL of 10^{-3} M aqueous $AgNO_3$ solution. Reduction of the Ag^+ ions was monitored by measuring the ultraviolet-visible spectrum of the solution at regular intervals on a spectrophotometer (SpectraMax M5, Molecular Devices Corporation, Sunnyvale, CA) operating at a resolution of 1 nm. The effects of temperature on the rate of synthesis and size of the prepared silver nanoparticles were studied by carrying out the reaction in a water bath at 4°C–50°C with reflux. The concentration of $AgNO_3$ solution was also varied from 0.3 to 5 mM.

TEM, HRTEM, and dynamic light scattering measurements
The surface morphology and size of the bioreduced silver nanoparticles was determined using a transmission electron microscope (TEM, Tecnai 12 Cryo, FEI, Eindhoven, The Netherlands). The morphology and size of the silver nanoparticles were also characterized by a higher resolution transmission electron microscope (HRTEM, JEOL-JEM-2100, Peabody, MA). Energy-dispersive spectra for the silver nanoparticles taken using an energy dispersive spectrometer

equipped with a JEOL JSM 6360A analytical scanning electron microscope at an energy range 0–20 keV confirmed the synthesis of silver nanoparticles using *D. bulbifera* tuber extract. The size of the particles in 3 mL of the reaction mixture was analyzed using dynamic light scattering equipment (Zetasizer Nano-2590, Malvern Instruments Ltd, Worcestershire, UK) in a polystyrene cuvette.

X-ray diffraction measurements

Phase formation of the bioreduced nanoparticles was studied using x-ray diffraction. Diffraction data for thin thoroughly dried nanoparticle films on glass slides were recorded on an x-ray diffractometer (D8 Advanced, Brucker, Germany) with a Cu Kα (1.54 Å) source.

Fourier transform infrared spectroscopy

A dry nanoparticle powder was obtained in the following manner. Silver nanoparticles synthesized after 5 hours of reaction of 1 mM AgNO3 solution with D. bulbifera tuber extract were centrifuged at 10,000 rpm for 15 minutes at room temperature, after which the pellet was redispersed in sterile distilled water. The process of centrifugation and redispersion in sterile distilled water was repeated three times to ensure better separation of free entities from the nanoparticles. The purified pellet was then dried and subjected to Fourier transform infrared (FTIR, IRAffinity-1, Shimadzu Corporation, Tokyo, Japan) spectroscopy measurement using the potassium bromide (KBr) pellet technique in diffuse reflection mode at a resolution of 4 cm^{-1}. The nanoparticle powder was mixed with KBr and exposed to an infrared source of 500–4000 cm^{-1}. A similar process was used for the FTIR study of *D. bulbifera* tuber extract before and after bioreduction.

Bactericidal activity and in combination

The effects of the silver nanoparticles synthesized using *D. bulbifera* tuber extract, standard antibiotics, and a combination of both were tested against both Gram-positive and Gram-negative bacterial strains using the disc diffusion method on Muller-Hinton agar plates. A single colony of

each test strain was grown overnight in liquid Muller-Hinton medium on a rotary shaker (200 rpm) at 37°C. The cells grown overnight were washed twice in sterile phosphate-buffered saline and the inocula were prepared by dilution with phosphate-buffered saline to a 0.4 McFarland standard and applied to plates along with the nanoparticles and standard antibiotics. For determination of the combined effect, discs containing 500 μg of different antibiotics were further impregnated with 5 μL of freshly prepared silver nanoparticles at a final concentration of 30 μg/disc. After incubation at 37°C for 18 hours, the zones of inhibition were measured. The assays were performed in triplicate.

Results
Phytochemical analysis

D. bulbifera is known to be rich in diverse phytochemicals like phenolics, flavonoids, carbohydrates, and vitamins that might play a significant role in the bioreduction of silver nanoparticles. Phytochemical analysis of *D. bulbifera* tuber extract revealed a high level of flavonoid content up to 4 mg/mL. Similarly, *D. bulbifera* tuber extract was found to be rich in phenolic content. Total reducing sugar was also found to be comparatively high (up to 3.41 mg/mL), followed by starch. *Dioscorea* is known to contain a saponin known as diosgenin. Table 1 shows the presence of diosgenin 26 μg/mL in *D. bulbifera* tuber extract. In addition to other phytochemicals, ascorbic acid and citric acid were detected in a range of 0.1–0.3 mg/mL.

### Synthesis of silver nanoparticles and optimization study

Bioreduction of Ag$^+$ to Ag^0 mediated by *D. bulbifera* tuber extract was monitored by recording the absorption spectra as a function of time. The well known yellowish-brown color of silver nanoparticles arises due to excitation of surface plasmon vibrations with an absorbance maxima at 450 nm (Figure 1). This might play a key role in the bioreduction process. A colloidal solution with development of intense brown coloration indicated the synthesis of silver nanoparticles, which showed a steady increase with time on shaking at 150 rpm and 40°C.

Table 1 Phytochemical content per mL of *Dioscorea bulbifera* tuber extract

Sample	Phytochemicals (mg/mL)						
	Total flavonoid content	Total phenolic content	Starch	Total reducing sugar	Diosgenin	Ascorbic acid	Citric acid
DBTE	4 ± 0.12	0.53 ± 0.04	1.08 ± 0.02	3.41 ± 0.15	0.026 ± 0.006	0.17 ± 0.005	0.28 ± 0.01

Note: Values are means ± standard deviation (n = 3).
Abbreviation: DBTE, *D. bulbifera* tuber extract.
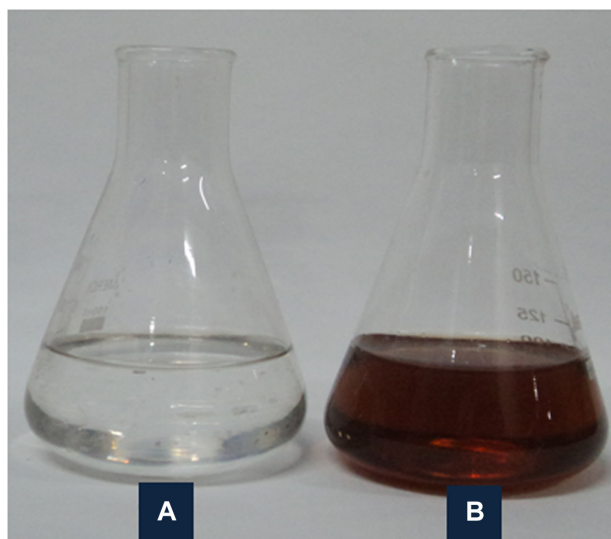
Figure 1 Solution of 1 mM AgNO$_3$ (**A**) before and (**B**) after bioreduction by *Dioscorea bulbifera* tuber extract at 40°C.

Ultraviolet-visible spectra of the reaction mixture of *D. bulbifera* tuber extract and AgNO$_3$ were recorded at regular time intervals (Figure 2). Although there was no significant synthesis at t = 0 minutes and t = 30 minutes, the rate of synthesis increased at t = 60 minutes at a very rapid rate and was completed in 5 hours. The silver nanoparticles formed employing *D. bulbifera* tuber extract were found to be very stable, possibly because of the starch present in the extract that prevented agglomeration, even after 30 days.

Optimization of the AgNO$_3$ concentration was carried out by plotting absorbance at the peak wavelengths of silver

nanoparticles against time. Variation in the reaction kinetics was observed at different concentrations (Figure 3). The rate of synthesis was found to be maximum at a concentration of 0.7 mM, while the higher concentrations had a comparatively low rate of bioreduction, with 0.3 mM showing the slowest rate of synthesis. Thus, the optimization study showed a significant effect of concentration on the synthesis of silver nanoparticles.

We further investigated the role of temperature on the reaction rate by varying the temperature from 4°C to 50°C. Maximal synthesis of silver nanoparticles was achieved at 50°C (Figure 4). The reaction was slow at lower temperatures, and no significant difference was found at 4°C, 20°C, and 30°C. However, an increase in the reaction rate was observed with an increase in temperature.

TEM, HRTEM, and energy dispersive spectrometry

The shape and size of the synthesized nanoparticles were elucidated with the help of TEM and HRTEM. The TEM images confirmed formation of silver nanoparticles (Figures 5 and 6). Formation of silver nanotriangles is a very rare event. The majority were formed as silver nanorods and triangles in the size range of 8–20 nm (Figure 5A). HRTEM images clearly show that the nanoparticles were mostly spherical in shape. Nanoparticles of larger dimensions (about 75 nm) were observed. TEM and HRTEM analysis also occasionally demonstrated hexagonal nanoparticles along with the triangles and rods
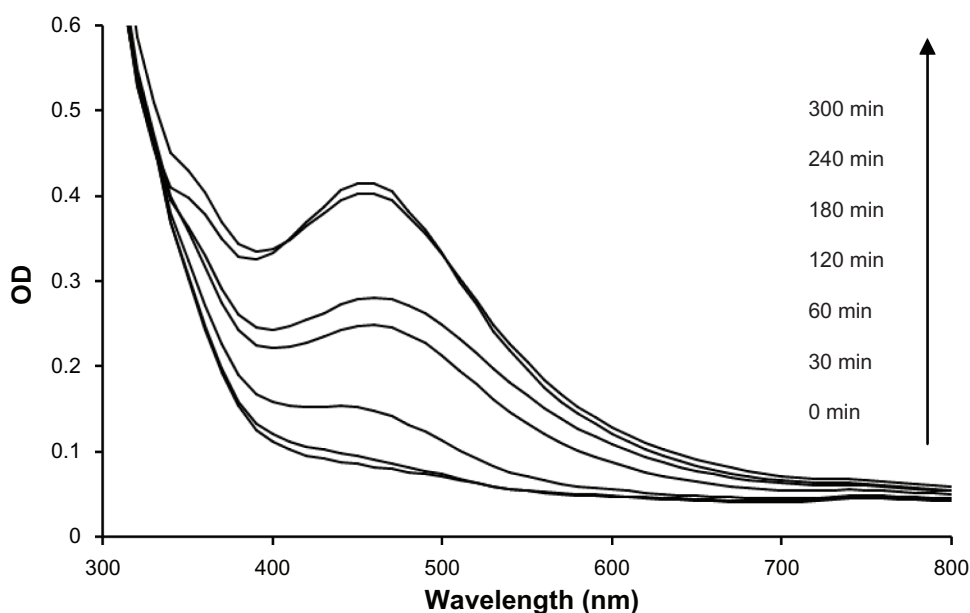

Figure 2 Ultraviolet-visible spectra recorded as a function of reaction time of 1 mM AgNO$_3$ solution with *Dioscorea bulbifera* tuber extract at 40°C.
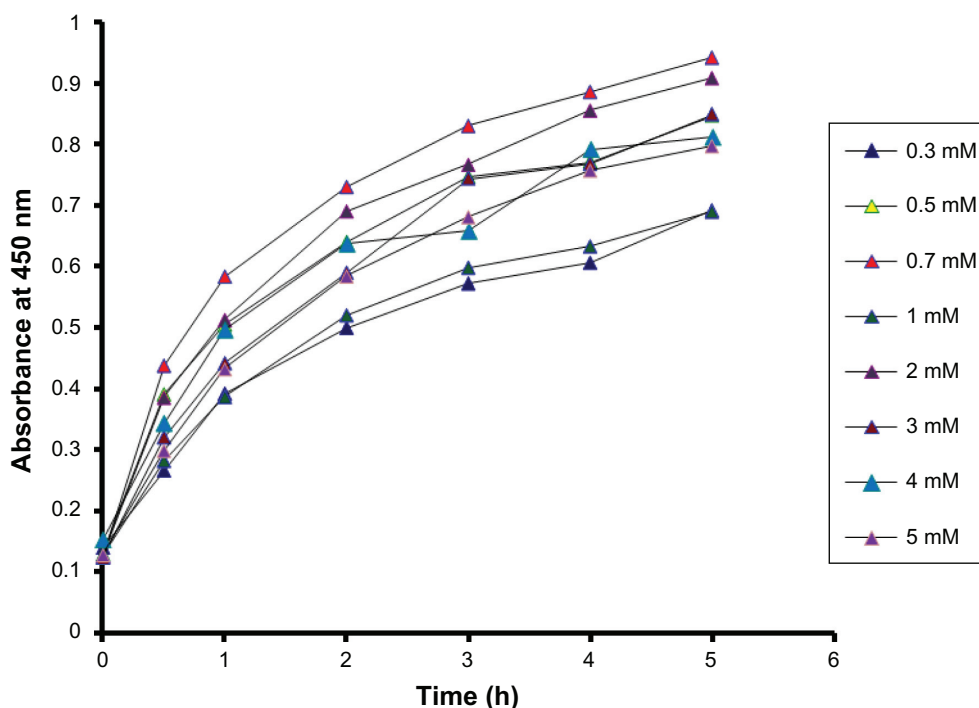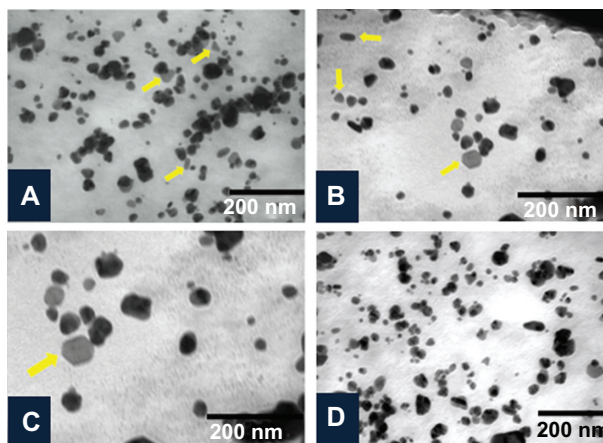
Figure 3 Time course of silver nanoparticles formation obtained with different concentrations of AgNO$_3$ using *Dioscorea bulbifera* tuber extract at 40°C.

(Figures 5C and 6D). The silver nanoparticles were anisotropic and included triangular, spherical, and ellipsoidal particles (Figure 5D, E, and F). The phytochemicals present in the tuber were believed to be the agents responsible for reducing the Ag$^+$ to Ag^0, but the shape is believed to be controlled by chemical factors like ascorbic acid and citric acid. Similarly, the starch content of *D. bulbifera* tuber extract may play a vital role in capping. Many triangular-shaped nanoparticles were observed in addition to the rods.

Energy dispersive x-ray spectroscopy results confirmed the presence of significant amounts of silver with no contaminants (Figure 7). The optical absorption peak was observed at approximately 3 keV, which is typical for the absorption of metallic silver nanocrystallites due to surface plasmon resonance. The particle size distribution of the silver nanoparticles determined by dynamic light scattering as shown in Figure 8 was found to be about 13.54 nm, which is well in agreement with the TEM analysis.
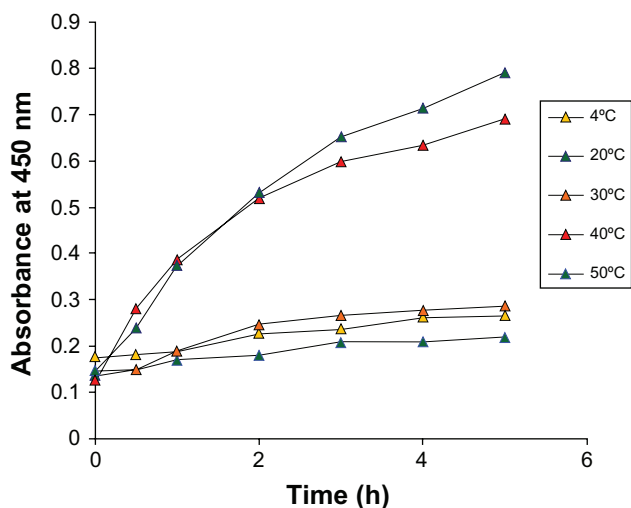
Figure 4 Time course of silver nanoparticles formation obtained with 1 mM AgNO$_3$ using *Dioscorea bulbifera* tuber extract with different reaction temperatures.

Figure 5 Characterization of silver nanoparticles formed with 1 mM AgNO$_3$ and 5% *Dioscorea bulbifera* tuber extract at 40°C by transmission electron microscopy. (**A**) Silver nanotriangles and nanorods, (**B**) anisotropic silver nanoparticles, (**C**), silver nanohexagon, and (**D**) irregular silver nanoparticles.
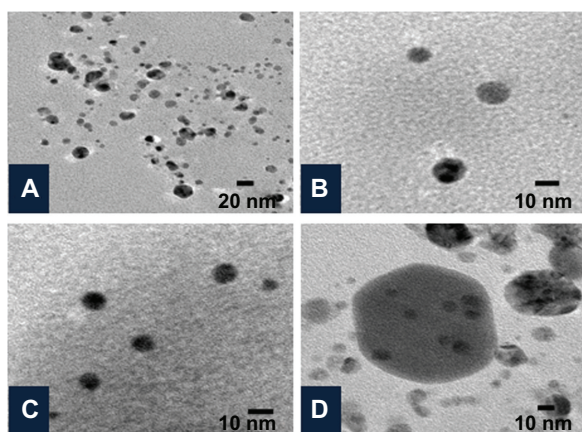
**Figure 6** Characterization of silver nanoparticles formed with 1 mM AgNO$_3$ and 5% *Dioscorea bulbifera* tuber extract at 40°C by high-resolution transmission electron microscopy. (**A**) Silver nanoparticles at a resolution of 20 nm, (**B** and **C**) spherical silver nanoparticles, and (**D**) Hexagonal silver nanoparticles.

X-ray diffraction analysis

The diffraction data for the dry powder were recorded on a Brucker x-ray diffractometer using a Cu Kα (1.54 Å) source. Phase formation was confirmed from characteristic peaks such as (111), (200), (220), and (311). The data matched with the standard Joint Committee for Powder Diffraction Set, Card 040783, confirming a face-centered cubic structure for the silver nanoparticles (Figure 9). The lack of any peaks resembling metal or metal oxide other than for pure silver in the diffraction data confirmed the purity of the synthesized silver nanoparticles. Broadening of the peak indicated a smaller particle size. The crystallite size was calculated using Scherrer's formula:

$$d = 0.9\lambda/\beta\cos$$

where 0.9 is the shape factor, generally taken for a cubic system, λ is the x-ray wavelength, typically 1.54 Å, β is the
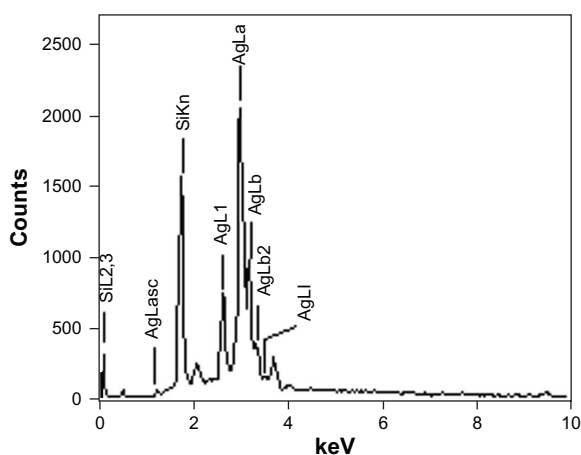
Figure 7 Representative spot energy-dispersive spectrometer profile confirming the presence of silver nanoparticles.

full width at half the maximum intensity in radians, and θ is the Bragg angle. Using the above formula, the calculated crystallite size was approximately 10 nm.

FTIR analysis

FTIR absorption spectra of *D. bulbifera* tuber extract before and after reduction of silver are shown in Figure 10. *D. bulbifera* tuber extract shows hydroxyl group in alcoholic and phenolic compound which is supported by the presence of a strong peak at approximately 3300 cm^{-1}. This sharp peak representing O—H bond is not seen in *D. bulbifera* tuber extract after bioreduction. This indicates that the polyols are mainly responsible for reduction of Ag$^+$ into silver nanoparticles. This may lead to the disappearance of the O—H bond. We could observe free hydroxyl groups in the FTIR of silver nanoparticles at 3600 cm^{-1}. The absorbance bands at 2931 cm^{-1}, 1625 cm^{-1}, 1404 cm^{-1}, and 1143 cm^{-1} are associated with the stretch vibrations of alkyl C—C, conjugated C—C with a benzene ring, bending of C—O—H and C—O stretch in saturated tertiary or secondary highly symmetric alcohol in *D. bulbifera* tuber extract, respectively. The presence of peaks at 3749 cm^{-1} and 1523 cm^{-1} indicate that the silver nanoparticles may be surrounded by amines, because the peaks indicate —NH$_2$ symmetric stretching and N—O bonds in nitro compounds.

Antimicrobial effects of antibiotics alone and combined with nanoparticles

Silver is well known as one of the most universal antimicrobial substances. The individual and combined effects of the bioreduced silver nanoparticles with 22 different antibiotics were investigated against 14 bacterial strains using the disc diffusion method. The diameter of the silver nanoparticle inhibition zones against different pathogenic cultures were observed (Table 2). Silver nanoparticles exhibited maximum cytotoxicity against *E. coli* and *Pseudomonas aeruginosa*, while moderate activity was found for *Salmonella typhi* and *Bacillus subtilis*. Silver nanoparticles were found to be comparatively less active in killing *Staphylococcus aureus*. Combined with the silver nanoparticles, the antibacterial activity of the antibiotics showed wide variation, not only between groups but also between members of the same group (Table 3). When combined with aminoglycosides, ie, amikacin and gentamicin, the silver nanoparticles showed comparable synergy (a 0.1–2.2-fold increase), and kanamycin was found to be superior against *P. aeruginosa*, showing a 4.2-fold enhancement in inhibition when used in combination. However, the best synergy was found with
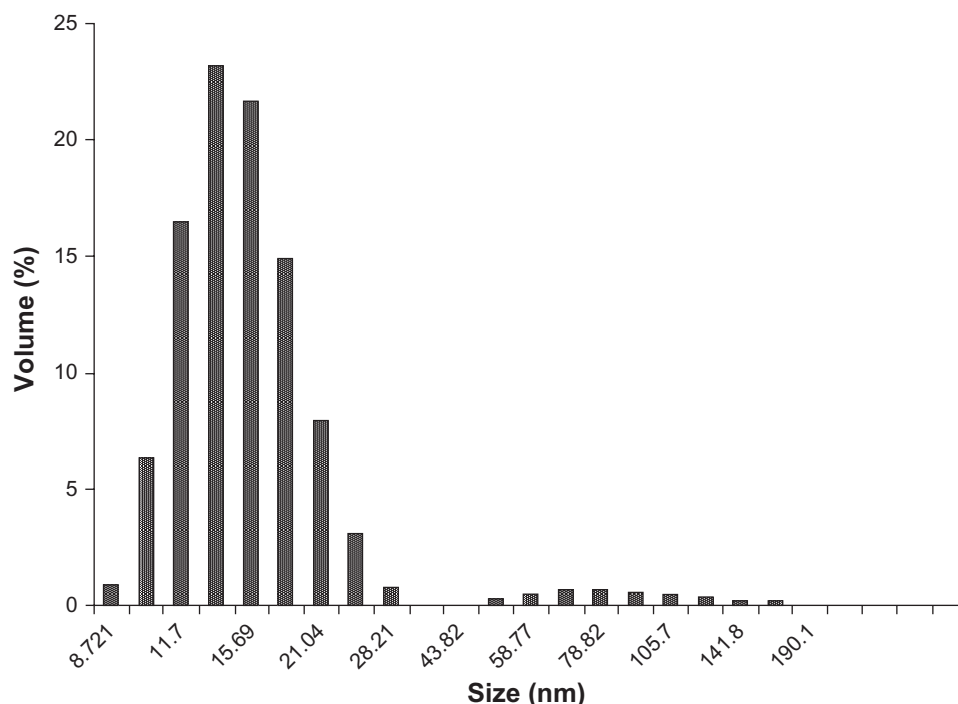
Figure 8 Histogram of size distribution of silver nanoparticles synthesized by *Dioscorea bulbifera* tuber extract.

streptomycin against *E. coli*, where inhibition increased by 11.8-fold. Among the β-lactams, the activity of ampicillin was enhanced against *Klebsiella pneumoniae*, *Neisseria mucosa*, and *P. aeruginosa*, with an appreciable increase in activity of 3–4.2-fold. On the other hand, the activity of penicillin was found to be enhanced moderately against *Acinetobacter baumannii*, *Enterobacter cloacae*, *P. aeruginosa*, *B. subtilis*, and *Pseudomonas koreensis*, and was highest against *K. pneumoniae*. It is important to note that the efficacy of piperacillin in combination with silver nanoparticles was selectively enhanced against *A. baumannii*

by up to 3.6-fold. Feropenem showed negligible or no synergy in combination with silver nanoparticles against any of the organisms tested, except for *K. pneumoniae*. Similarly, in the cephalosporin group of antibiotics, synergy was observed only for ceftazidime against *E. coli*. Polymyxin, a cyclic peptide antibiotic, showed negligible variation in activity whether used alone or in combination with silver nanoparticles against all the test pathogens. Even Gram-negative bacteria like *K. pneumoniae*, *Proteus mirabilis*, and *P. aeruginosa*, were found to be inhibited in the presence of a combination of vancomycin and silver nanoparticles,
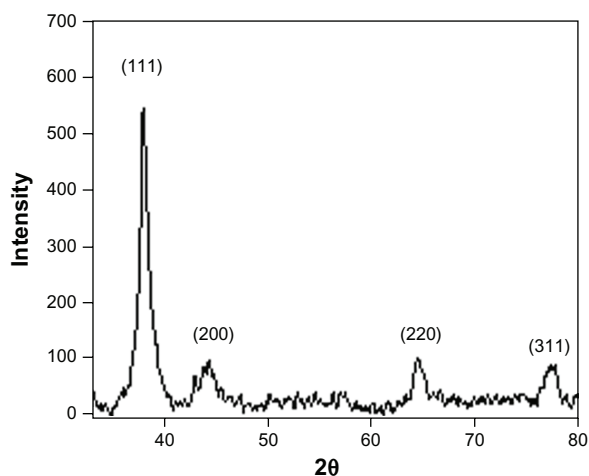
Figure 9 Representative x-ray diffraction profile of thin film silver nanoparticles.
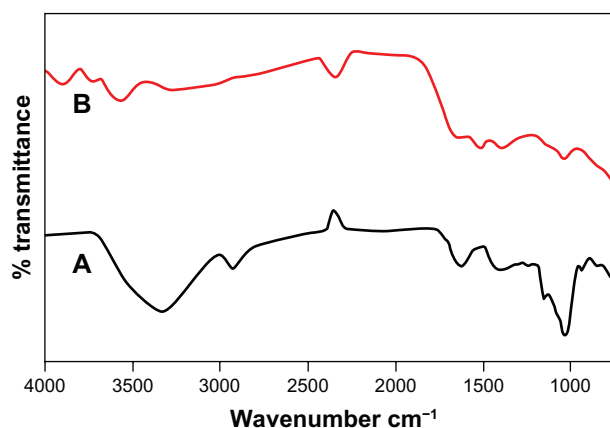
Figure 10 Fourier transform infrared absorption spectra of dried *Dioscorea bulbifera* tuber extract (**A**) before bioreduction and (**B**) after complete bioreduction of Ag+ ions at 50°C.

which otherwise showed a resistant pattern in the presence of the antibiotic alone. Erythromycin showed enhanced activity of 1.5–3.0-fold against *K. pneumoniae*, *P. mirabilis*, *P. aeruginosa*, *S. typhi*, and *A. baumannii* in combination with silver nanoparticles. Silver nanoparticles increased the efficacy of nalidixic acid, a member of the quinolone group of antibiotics, against both Gram-positive and Gram-negative microbes, in particular *E. coli* and *P. koreensis*. Rifampicin and tetracyclines showed identical activity in the presence and absence of silver nanoparticles against most of the tested pathogens. The activity of chloramphenicol against *P. aeruginosa* was remarkably enhanced by up to 4.9-fold in the presence of silver nanoparticles, but moderate synergy was observed against the other Gram-positive pathogens tested. Combination of silver nanoparticles with nitrofurantoin and trimethoprim showed identical selective synergistic efficacy against *K. pneumoniae*.

Discussion

We have successfully demonstrated a rapid and efficient route for synthesis of silver nanoparticles using *D. bulbifera* tuber extract. The development of intense yellowish brown color owing to the surface plasmon resonance confirmed the synthesis of the silver nanoparticles.[10] *D. bulbifera* tuber is a rich source of flavonoids and phenolic acid derivatives.[36,26] Flavonoids play a vital role in the reduction process for synthesis of nanoparticles.[37] Thus, the high flavonoid and phenolic content in *D. bulbifera* tuber extract revealed in the phytochemical analysis strongly supports the potential of *D. bulbifera* tuber extract to bioreduce Ag^+ to Ag^0. Similarly, the reducing sugars that are known to play a vital role in bioreduction were found to be predominant in *D. bulbifera* tuber extract.[38] It is important to note that *D. bulbifera* contains ascorbic acid and citric acid in notable amounts.[39,40] This is in agreement with the presence of both ascorbic and citric acid in *D. bulbifera* tuber extract in our study as well. Widespread use of ascorbic and citric acid in the synthesis of silver nanoparticles provides a strong rationale for use of *D. bulbifera* tuber extract in the synthesis and shaping of silver nanoparticles.[41–43] Diosgenin is reported to be a predominant saponin in *D. bulbifera*[39,44] which might contribute to the surfactant properties of *D. bulbifera* tuber extract. Plant surfactants are widely used in the synthesis of silver nanoparticles.[45] Likewise, the significant starch content in *D. bulbifera* tuber extract reflects the capping properties of the extract, and starch is widely used in various synthetic processes for capping and stabilizing silver nanoparticles.[46] Thus, phytochemical studies support the use

of *D. bulbifera* tuber extract as a suitable agent to facilitate the synthesis of silver nanoparticles. The complete reduction of Ag^+ within 5 hours indicates that synthesis was much faster as compared with other plants like *Sesuvium portulacastrum* L that take 24 hours for complete synthesis of silver nanoparticles to occur.[47] Optimization studies showed that the sharpness of the peak increased with an increase in temperature. Most likely, this occurs due to an increase in the reaction rate of conversion of metal ions to nanoparticles at higher temperatures.[48] Recently, different plant systems have been used to synthesize spherical and irregular silver nanoparticles.[47] Although nanospheres dominated the population of the synthesized silver nanoparticles as evident from HRTEM and TEM micrographs, in some cases anisotropy was observed similar to other reports.[49] Anisotropy among the silver nanoparticles could be related to the recent report by Huang et al mentioning that nascent silver crystals formed using *Cinnamomum camphora* leaf powder were gradually enclosed by protective molecules, which as a result eliminated rapid sintering of smaller nanoparticles, resulting in formation of nanotriangles.[12] The spot energy-dispersive spectrometry data confirmed the purity of the metallic nanosilver, while the particle size was calculated to be approximately 10 nm from the x-ray diffraction data.[50,51] The FTIR absorption spectra offered information regarding chemical changes in the functional groups involved in bioreduction.[52] *D. bulbifera* tubers are known to contain various bioactive compounds, including flavonoids, terpenoids, phenanthrenes, amino acids, protein, and glycosides.[53–59] It is speculated that the alcohol groups are oxidized to carbonyl groups in the course of reduction, which supports the suggestion that polyol groups are primarily responsible for the bioreduction process. Thus, the water-soluble fractions of *D. bulbifera* played key roles in the bioreduction of the precursors and evolution of shape in the nanoparticles.

Silver ion and silver-based compounds are highly toxic to micro-organisms, showing a strong biocidal effect against microbial species because these are highly reactive species with a large surface area.[60–63] Silver nanoparticles produced using microbes and plant extracts are known to exhibit potent antimicrobial activity.[47] Antimicrobial activity determined using the disc diffusion method confirmed that combining antibiotics with silver nanoparticles resulted in a greater bactericidal effect on the test pathogens than either of the antibacterial agents used alone. This experiment provides solid evidence of the antibacterial synergy between antibiotics and silver nanoparticles. A very interesting observation

Table 2 Zone of inhibition (mm) of different concentrations of silver nanoparticles on the test pathogens by disc diffusion method

AgNPs µg/disc	Zone diameter (mm)						
	Acinetobacter baumannii	*Enterobacter cloacae*	*Escherichia coli*	*Haemophilus influenzae*	*Klebsiella pneumoniae*	*Neisseria mucosa*	*Proteus mirabilis*
1000	13	12	18	12	16	21	NI
500	12	10	15	11	15	20	NI
300	11	8	14	9	14	18	NI
100	10	NI	13	8	12	16	NI
50	8	NI	12	NI	11	15	NI
30	NI	NI	10	NI	9	14	NI
20	NI	NI	9	NI	8	12	NI
10	NI	NI	NI	NI	NI	10	NI

Table 3 Zone of inhibition (mm) of different antibiotics against test strains in absence and in presence of silver nanoparticles (30 µg/disc)

Antiboitics	*Acinetobacter baumannii*			*Enterobacter cloacae*			*Escherichia coli*			*Haemophilus influenzae*			*Klebsiella pneumoniae*			*Neisseria mucosa*			*Proteus mirabilis*		
	A	B	C	A	B	C	A	B	C	A	B	C	A	B	C	A	B	C	A	B	C
Aminoglycosides																					
Amikacin	23.0	23.0	0.0	19.0	20.0	0.1	10.0	18.0	2.2	23.0	23.0	0.0	17.0	17.0	0.0	20.0	26.0	0.7	17.0	17.0	0.0
Gentamycin	13.0	14.0	0.2	17.0	17.0	0.0	17.0	17.0	0.0	23.0	23.0	0.0	18.0	18.0	0.0	30.0	42.0	1.0	20.0	20.0	0.0
Kanamycin	7.0	10.0	1.0	18.0	18.0	0.0	14.0	16.0	0.3	22.0	22.0	0.0	7.0	9.0	0.7	26.0	26.0	0.0	17.0	17.0	0.0
Streptomycin	16.0	16.0	0.0	23.0	23.0	0.0	7.0	25.0	11.8	24.0	24.0	0.0	22.0	22.0	0.0	28.0	28.0	0.0	20.0	20.0	0.0
β-Lactams																					
Amoxicillin	7.0	9.0	0.7	7.0	8.0	0.3	12.0	12.0	0.0	10.0	10.0	0.0	7.0	10.0	1.0	40.0	40.0	0.0	16.0	16.0	0.0
Ampicillin	7.0	12.0	1.9	14.0	14.0	0.0	29.0	29.0	0.0	10.0	10.0	0.0	7.0	15.0	3.6	22.0	50.0	4.2	7.0	7.0	0.0
Penicillin	7.0	13.0	2.4	7.0	12.0	1.9	10.0	10.0	0.0	13.0	13.0	0.0	7.0	16.0	4.2	46.0	48.0	0.1	14.0	14.0	0.0
Piperacillin	7.0	15.0	3.6	18.0	0.0	15.0	15.0	15.0	0.0	17.0	17.0	0.0	18.0	18.0	0.0	40.0	40.0	0.0	18.0	18.0	0.0
Carbapenem																					
Feropenem	17.0	17.0	0.0	13.0	13.0	0.0	18.0	18.0	0.0	25.0	25.0	0.0	7.0	15.0	3.6	48.0	48.0	0.0	15.0	15.0	0.0
Cephalosporin																					
Ceftazidime	8.0	8.0	0.0	20.0	20.0	0.0	9.0	18.0	3.0	17.0	17.0	0.0	9.0	9.0	0.0	32.0	32.0	0.0	20.0	20.0	0.0
Ceftriaxone	11.0	11.0	0.0	20.0	20.0	0.0	7.0	7.0	0.0	13.0	15.0	0.3	16.0	16.0	0.0	47.0	47.0	0.0	18.0	18.0	0.0
Cefotaxime	10.0	130	0.7	23.0	23.0	0.0	7.0	7.0	0.0	14.0	17.0	0.5	16.0	16.0	0.0	30.0	30.0	0.0	15.0	15.0	0.0
Cyclic peptide																					
Polymyxin	15.0	15.0	0.0	13.0	13.0	0.0	7.0	8.0	0.3	10.0	10.0	0.0	16.0	16.0	0.0	16.0	18.0	0.3	7.0	7.0	0.0
Glycopeptides																					
Vancomycin	12.0	12.0	0.0	7.0	7.0	0.0	18.0	19.0	0.1	23.0	23.0	0.0	7.0	13.0	2.4	24.0	25.0	0.1	7.0	12.0	1.9
Macrolide																					
Erythromycin	7.0	14.0	3.0	7.0	8.0	0.3	7.0	8.0	0.3	18.0	18.0	0.0	7.0	11.0	1.5	25.0	27.0	0.2	7.0	11.0	1.5
Quinolones																					
Nalidixic acid	7.0	10.0	1.0	11.0	12.0	0.2	7.0	140	3.0	8.0	8.0	0.0	7.0	7.0	0.0	14.0	14.0	0.0	7.0	9.0	0.7
Rifamycin																					
Rifampicin	20.0	20.0	0.0	13.0	13.0	0.0	15.0	15.0.	0.0.	16.0	16.0	0.0	10.0	15.3	1.3	44.0	44.0	0.0.	15.0	15.0	0.0
Tetracycline																					
Tetracycline	17.0	17.0	0.0	21.0	21.0	0.0	27.0	27.0	0.0	25.0	25.0	0.0	18.0	18.0	0.0	34.0	38.0	0.2	18.0	18.0	0.0
Doxycycline	21.0	21.0	0.0	18.0	18.0	0.0	12.0	12.0	0.0	24.0	24.0	0.0	13.0	13.0	0.0	34.0	34.0	0.0	10.0	10.0	0.0
Others																					
Chloramphenicol	10.0	10.0	0.0	22.0	22.0	0.0	26.0	26.0	0.0	17.0	17.0	0.0	7.0	12.0	1.9	32.0	32.0	0.0	16.0	16.0	0.0
Nitrofurantoin	7.0	11.0	1.5	9.0	9.0	0.0	8.0	8.0	0.0	10.0	12.0	0.4	7.0	16.0	4.2	8.0	31.0	14.0	9.0	9.0	0.0
Trimethoprim	7.0	11.0	1.5	16.0	16.0	0.0	16.0	170	0.1	7.0	13.0	2.4	7.0	16.0	4.2	25.0	26.0	0.1	7.0	7.0	0.0

Pseudomonas aeruginosa	*Salmonella typhi*	*Serratia odorifera*	*Vibrio parahaemolyticus*	*Bacillus subtilis*	*Paenibacillus koreensis*	*Staphylococcus aureus*
10	12	10	12	17	12	8
9	11	9	11	16	11	7
8	10	8	9	15	9	NI
NI	9	NI	8	13	8	NI
NI	NI	NI	NI	11	NI	NI
NI	NI	NI	NI	10	NI	NI
NI	NI	NI	NI	9	NI	NI
NI	NI	NI	NI	NI	NI	NI

Note: All experiments were performed in triplicate, and standard deviations were negligible.
Abbreviations: NI, no inhibition; AgNPs, silver nanoparticles.

Pseudomonas aeruginosa			*Salmonella typhi*			*Serratia odorifera*			*Vibrio parahaemolyticus*			*Bacillus subtilis*			*Paenibacillus koreensis*			*Staphylococcus aureus*		
A	B	C	A	B	C	A	B	C	A	B	C	A	B	C	A	B	C	A	B	C
14.0	22.0	1.5	7.0	8.0	0.3	20.0	20.0	0.0	24.0	24.0	0.0	20.0	20.0	0.0	15.0	20.0	0.8	11.0	15.0	0.9
27.0	27.0	0.0	7.0	9.0	0.7	26.0	26.0	0.0	30.0	30.0	0.0	20.0	20.0	0.0	20.0	22.0	0.2	17.0	17.0	0.0
7.0	16.0	4.2	7.0	10.0	1.0	26.0	26.0	0.0	22.0	23.0	0.1	23.0	23.0	0.0	20.0	22.0	0.2	16.0	17.0	0.1
24.0	32.0	0.8	7.0	10.0	1.0	23.0	23.0	0.0	30.0	30.0	0.0	26.0	37.0	0.1	23.0	23.0	0.0	16.0	18.0	0.3
7.0	12.0	1.9	7.0	12.0	1.9	20.0	20.0	0.0	11.0	11.0	0.0	10.0	10.0	0.0	7.0	10.0	1.0	7.0	10.0	1.0
8.0	16.0	3.0	20.0	27.0	0.8	27.0	27.0	0.0	13.0	14.0	0.2	20.0	34.0	1.9	11.0	13.0	0.4	18.0	19.0	0.1
7.0	13.0	2.4	18.0	24.0	0.8	20.0	20.0	0.0	15.0	15.0	0.0	7.0	11.0	1.5	7.0	11.0	1.5	15.0	15.0	0.0
26.0	26.0	0.0	15.0	18.0	0.4	24.0	24.0	0.0	20.0	20.0	0.0	10.0	14.0	1.0	7.0	15.0	1.3	15.0	15.0	0.0
12.0	13.0	0.0	14.0	14.0	0.0	25.0	25.0	0.0	30.0	30.0	0.0	34.0	34.0	0.0	22.0	23.0	0.1	18.0	18.0	0.0
20.0	20.0	0.0	16.0	16.0	0.0	24.0	25.0	0.1	20.0	20.0	0.0	21.0	21.0	0.0	16.0	17.0	0.1	12.0	150	0.6
18.5	18.5	0.0	15.0	18.0	0.4	24.0	24.0	0.0	15.0	18.0	0.4	14.0	14.0	0.0	15.0	15.0	0.0	17.0	17.0	0.0
15.0	15.0	0.0	18.0	20.0	0.2	25.0	25.0	0.0	16.0	18.0	0.3	15.0	16.0	0.1	18.0	18..0	0.0	20.0	20.0	0.0
14.0	14.0	0.0	7.0	8.0	0.3	14.0	14.0	0.0	11.0	14.0	0.6	7.0	9.0	0.7	11.0	12.0	0.2	7.0	8.0	0.3
7.0	16.0	4.2	18.0	22.0	0.5	7.0	8.0	0.3	23.0	23.0	0.0	24.0	25.0	0.0	18.0	18.0	0.0	15.0	15.0	0.0
7.0	13.0	2.4	7.0	13.0	2.4	7.0	8.0	0.3	20.0	20.0	0.0	19.0	19.0	0.0	16.0	20.0	0.6	7.0	8.0	0.3
7.0	13.0	2.4	8.0	10.0	0.6	9.0	14.0	1.4	11.0	12.0	0.2	9.0	12.0	0.8	7.0	13.0	2.4	7.0	11.0	1.5
15.0	15.0	0.0	21.0	21.0	0.0	13.0	13.0	0.0	18.0	18.0	0.0	16.0	16.0	0.0	17.0	17.0	0.0	7.0	7.0	0.0
19.0	20.0	0.1	17.0	20.0	0.4	21.0	22.0	0.1	25.0	25.0	0.0	30.0	39.0	0.7	22.0	24.0	0.2	25.0	25.0	0.0
11.0	12.0	0.2	21.0	21.0	0.0	20.0	20.0	0.0	28.0	28.0	0.0	19.0	19.0	0.0	19.0	20.0	0.1	11.0	11.0	0.0
7.0	17.0	4.9	22.0	24.0	0.2	22.0	22.0	0.0	21.0	21.0	0.0	24.0	32.0	0.8	23.0	25.0	0.2	7.0	10.0	1.0
7.0	11.0	1.5	7.0	9.0	0.7	7.0	8.0	0.3	13.0	19.0	1.1	11.0	20.0	2.3	7.0	13.0	2.4	7.0	7.0	0.0
7.0	11.0	1.5	7.0	7.0	0.0	7.0	13.0	2.4	7.0	15.0	3.6	7.0	20.0	7.2	7.0	13.0	2.4	7.0	10.0	1.0

Notes: All experiments were done in triplicate, and standard deviations were negligible. Fold increases (C) for different antibiotics against five bacterial pathogens were calculated as $(B^2 - A^2)/A^2$, where A and B are the inhibition zones in mm for antibiotic only and antibiotic in combination with silver nanoparticles, respectively. In the absence of bacterial growth inhibition zones, the disk diameters (7 mm) were used to calculate the fold increase (C).
Abbreviation: AgNPs, silver nanoparticles.

that *A. baumannii*, a nosocomial pathogen resistant to almost all known antibiotics and metal salts commonly used in medicine, could also be sensitized in the presence of silver nanoparticles.[64–67] Therefore, this combinational approach of antibiotics and silver nanoparticles would provide a strategy for effective control of *A. baumannii.* From the results, we can conclude that the antimicrobial effect of silver nanoparticles is the key contributor to the synergistic effect observed with a combination of silver nanoparticles and antibiotics.

Scientists have established the antibacterial mechanism of β-lactams, chloramphenicol, aminoglycosides, tetracyclines, and glycopeptides.[68,69] However, there has not been a consistent explanation for the antimicrobial mechanism of silver, although application of silver to burn wounds has been done for more than a century.[70] This can be attributed to the fact that silver at low concentrations does not enter cells, but is adsorbed onto the bacterial surface just as silver tends to adsorb to other surfaces.[67] Thus, silver ions resist dehydrogenation because respiration occurs across the cell membrane in bacteria rather than across the mitochondrial membrane as in eukaryotic cells.[71] Again, some hypotheses indicate that catalytic oxidation of silver ions, with nascent oxygen, reacts with bacterial cell membranes, leading to cell death. A pronounced antimicrobial effect of antibiotics in combination with silver nanoparticles was observed in this study. This clearly indicates that enhancement of efficacy was due to the synergistic antibacterial action between antibiotics and silver nanoparticles. As discussed above, silver nanoparticles and antibiotics can kill bacteria with a different mechanism. Thus, the synergistic effect can act as a very powerful tool against resistant micro-organisms. A bonding reaction between antibiotics and silver nanoparticles by chelation ultimately increases the concentration of antimicrobial agents at specific points on the cell membrane. This may be attributed due to the selective approach of silver nanoparticles towards the cell membrane that consists of phospholipids and glycoprotein. Therefore, silver nanoparticles facilitate the transport of antibiotics to the cell surface acting as a drug carrier. As the silver nanoparticles bind to the sulfur-containing proteins of the bacterial cell membrane, the permeability of the membrane increases, facilitating enhanced infiltration of the antibiotics into the cell. More recently, it was shown that silver (I) chelation prevents unwinding of DNA. Silver nanoparticles are composed of silver (0) atoms.[72] Silver nanoparticles are larger in size than silver (I) ions, which makes them react with more molecules, leading to more antimicrobial activity.

Conclusion

In an attempt to find natural, environmentally benign, and easily available plant-based agents for synthesis of metal nanoparticles, we have demonstrated for the first time the efficiency of *D. bulbifera* tuber extract in the rapid synthesis of stable silver nanoparticles possessing a variety of fascinating morphologies owing to its diverse groups of phytochemicals like phenolics, flavonoids, reducing sugars, ascorbic acid, citric acid, and diosgenin. Based on our kinetic studies, together with evidence obtained from FTIR, we propose that the main biomolecules responsible for nanoparticle synthesis were polyphenols or flavonoids. The results of our study show that the combination of silver nanoparticles and antibiotics had synergistic antibacterial efficiency against the test microbes, particularly *P. aeruginosa*, *E. coli*, and *A. baumannii*. To elucidate the mechanism of this synergistic antibacterial effect, more elaborate experimental evidence will be required. Overall, this combinational approach of antibiotic and silver nanoparticles seems to be one of the best strategies for control of antibiotic-resistant micro-organisms and hence therapeutic management in infection control.

Acknowledgment

Disclosure
The authors report no conflicts of interest in this work.

References
1. Gittins DI, Bethell D, Schiffrin DJ, Nichols RJ. A nanometre-scale electronic switch consisting of a metal cluster and redox-addressable groups. *Nature*. 2000;408(6808):67–69.
2. Darroudi M, Ahmad MB, Abdullah AH, Ibrahim NA. Green synthesis and characterization of gelatin-based and sugar-reduced silver nanoparticles. *Int J Nanomedicine*. 2011;6:569–574.
3. Wise K, Brasuel M. The current state of engineered nanomaterials in consumer goods and waste streams: the need to develop nanoproperty-quantifiable sensors for monitoring engineered nanomaterials. *Nanotechnol Sci Appl*. 2011;4:73–86.
4. Mukherjee P, Roy M, Mandal BP, et al. Green synthesis of highly stabilized nanocrystalline silver particles by a non-pathogenic and agriculturally important fungus *T. asperellum*. *Nanotechnology*. 2008;19(7):075103–075110.
5. Ai J, Biazar E, Jafarpour M, et al. Nanotoxicology and nanoparticle safety in biomedical designs. *Int J Nanomedicine*. 2011;6:1117–1127.
6. Sastry M, Ahmad A, Khan MI, Kumar R. Biosynthesis of metal nanoparticles using fungi and actinomycete. *Curr Sci*. 2003;85(2):162–170.
7. Shankar SS, Rai A, Ankamwar B, Singh A, Ahmad A, Sastry M. Biological synthesis of triangular gold nanoprisms. *Nat Mater*. 2004;3(7):482–488.
8. Binupriya AR, Sathishkumar M, Yun SI. Myco-crystallization of silver ions to nano-sized particles by live and dead cell filtrates of *Aspergillus oryzae* var viridis and its bactericidal activity towards *Staphylococcus aureus* KCCM 12256. *Ind Eng Chem Res*. 2010;49(2):852–858.

9. Shankar SS, Rai A, Ahmad A, Sastry M. Controlling the optical properties of lemongrass extract synthesized gold nanotriangles and potential application in infrared-absorbing optical coatings. *Chem Mater*. 2005;17(3):566–572.

10. Shankar SS, Rai A, Ankamwar B, Ahmad A, Sastry M. Rapid synthesis of Au, Ag, and bimetallic Au-core-Ag shell nanoparticles using neem (*Azadirachta indica*) leaf broth. *J Colloid Interface Sci*. 2004;275(2):496–502.

11. Shankar SS, Ahmad A, Sastry M. Geranium leaf assisted biosynthesis of silver nanoparticles. *Biotechnol Prog*. 2003;19(6):1627–1631.

12. Huang J, Li Q, Sun D, et al. Biosynthesis of silver and gold nanoparticles by novel sundried *Cinnanonumcamphora* leaf. *Nanotechnology*. 2007;18(10):105104–105114.

13. Elavazhagan T, Arunachalam KD. *Memecylon edule* leaf extract mediated green synthesis of silver and gold nanoparticles. *Int J Nanomedicine*. 2011;6:1265–1278.

14. Ankamwar B, Damle C, Ahmad A, Sastry M. Biosynthesis of gold and silver nanoparticles using *Emblica officinalis* fruit extract, their phase transfer and transmetallation in an organic solution. *J Nanosci Nanotechnol*. 2005;5(10):1665–1671.

15. Panacek A, Kvitek L, Prucek R, et al. Silver colloid nanoparticles: synthesis, characterization, and their antibacterial activity. *J Phys Chem B*. 2007;110(33):16248–16253.

16. Neu HC. Crisis of antibiotic resistance. *Science*. 1992;257(5073): 1064–1073.

17. Pitout JDD, Sanders CC, Sanders WE. Antimicrobial resistance with focus on β-lactam resistance in Gram-negative bacilli. *Am J Med*. 1997; 103(1):51–59.

18. Craig WA. Antimicrobial resistance issues of the future. *Diagn Microbiol Infect Dis*. 1996;25(4):213–217.

19. Shakibaie MR, Dhakephalkar PK, Kapadnis BP, Chopade BA. Removal of silver from photographic wastewater effluent using *Acinetobacter baumannii* BL54. *Can J Microbiol*. 1999;45(12):995–1000.

20. Patwardhan RB, Dhakephalkar PK, Niphadkar KB, Chopade BA. Incidence and prevalence of nosocomial pathogens in ICU with special reference to multiresistant *Acinetobacter baumannii* harboring multiple plasmids. *Indian J Med Res*. 2008;128(8):178–187.

21. Sondi I, Salopek-Sondi B. Silver nanoparticles as antimicrobial agent: a case study on *E. coli* as a model for gram-negative bacteria. *J Colloid Interface Sci*. 2004;275(1):177–182.

22. Shi Z, Neoh KG, Kang ET. Surface-grafted viologen for precipitation of silver nanoparticles and their combined bactericidal activities. *Langmuir*. 2004;20(16):6847–6852.

23. Choi HJ, Han SW, Lee SJ, Kim K. Structure and thermal behavior of a layered silver hydroxyalkanecarboxylate. *J Colloid Interface Sci*. 2003;264(2):458–466.

24. Sautour M, Mitaine-Offer AC, Lacaille-Dubois MA. The Dioscorea genus: a review of bioactive steroid saponins. *J Nat Med*. 2007;61(2):91–101.

25. Gao H, Kuroyanagi M, Wu L, Kawahara N, Yasuno T, Nakamura Y. Antitumor-promoting constituents from *D. bulbifera* L. in JB6 mouse epidermal cells. *Biol Pharm Bull*. 2002;25(9):1241–1243.

26. Bhandari MR, Kawabata J. Organic acid, phenolic content and antioxidant activity of wild yam (*Dioscorea*. spp.) tubers of Nepal. *Food Chem*. 2004;88(2):163–168.

27. Ghosh S, Ahire M, Patil S, et al. Antidiabetic activity of *Gnidia glauca* and *Dioscorea bulbifera*: Potent amylase and glucosidase inhibitors. *Evid Based Complement Alternat Med*. 2011; 2012(2012):929051.

28. Ghosh S, Patil S, Ahire M, et al. Synthesis of gold nano-anisotrops using *Dioscorea bulbifera* tuber extract. *J Nanomater*. 2011:2011.

29. Luximon-Ramma A, Bahorun T, Soobrattee MA, Aruoma OI. Antioxidant activities of phenolic, proanthocyanidin, and flavonoid components in extracts of *Cassia fistula*. *J Agric Food Chem*. 2002;50(18):5042–5047.

30. Wolfe K, Wu X, Liu RH. Antioxidant activity of apple peels. *J Agric Food Chem*. 2003;51(3):609–614.

31. Thayumanavan B, Sadasivam S. Physicochemical basis for the preferential uses of certain rice varieties. *Qual Plant Foods Hum Nutr*. 1984;34(4):253–257.

32. Miller GL. Use of dinitrosalicylic acid reagent for determination of reducing sugar. *Anal Chem*. 1959;31(3):426–428.

33. Slack SC, Mader WJ. Colorimetric assay for diosgenin and related compounds. *Anal Chem*. 1961;33(4):625–627.

34. Sadasivam S, Manickam A. *Biochemical Methods*. 3rd ed. New Delhi, India: New Age International; 2008.

35. Saffran M, Denstedt OF. A rapid method for the determination of citric acid. *J Biol Chem*. 1948;175:849–855.

36. Gao H, Hou B, Kuroyanagi M, Wu L. Constituents from anti-tumor-promoting active part of *Dioscorea bulbifera* L. in JB6 mouse epidermal cells. *Asian J Tradit Med*. 2007;2(3):104–109.

37. Egorova EM, Revina AA. Synthesis of metallic nanoparticles in reverse micelles in the presence of quercetin. *Colloids Surf A Physicochem Eng Asp*. 2000;168(1):87–96.

38. Panigrahi S, Kundu S, Ghosh SK, Nath S, Pal T. General method of synthesis for metal nanoparticles. *J Nanopart Res*. 2004;6(4): 411–414.

39. Behera KK, Sahoo S, Prusti A. Biochemical quantification of diosgenin and ascorbic acid from the tubers of different dioscorea species found in Orissa. *Lib Agric Res Cent J Int*. 2010;1(2):123–127.

40. Suriyavathana M, Indupriya S. Screening of antioxidant potentials in *Dioscorea bulbifera*. *Int J Pharm Life Sci*. 2011;2(4):661–664.

41. Qin Y, Ji X, Jing J, Liu H, Wu H, Yang W. Size control over spherical silver nanoparticles by ascorbic acid reduction. *Colloids Surf A Physicochem Eng Asp*. 2010;372(1–3):172–176.

42. Lee GP, Bignell LJ, Romeo TC, et al. The citrate-mediated shape evolution of transforming photomorphic silver nanoparticles. *Chem Commun*. 2010;46(41):7807–7809.

43. Dong X, Ji X, Wu H, Zhao L, Li J, Yang W. Shape control of silver nanoparticles by stepwise citrate reduction. *J Phys Chem C*. 2009; 113(16):6573–6576.

44. Guclu-Ustundag O, Mazza G. Saponins: properties, applications and processing. *Crit Rev Food Sci Nutr*. 2007;47(3):231–258.

45. Nadagouda MN, Hoag G, Collins J, Varma RS. Green synthesis of Au nanostructures at room temperature using biodegradable plant surfactants. *Cryst Growth Des*. 2009;9(11):4979–4983.

46. Sharma VK, Yngard RA, Lin Y. Silver nanoparticles: Green synthesis and their antimicrobial activities. *Adv Colloid Interface Sci*. 2009; 145(1–2):83–96.

47. Nabikhan A, Kandasamy K, Raj A, Alikunhi NM. Synthesis of antimicrobial silver nanoparticles by callus and leaf extracts from saltmarsh plant, *Sesuvium portulacastrum* L. *Colloids Surf B Biointerfaces*. 2010;79(2):488–493.

48. Song JY, Kim BS. Rapid biological synthesis of silver nanoparticles using plant leaf extracts. *Bioprocess Biosyst Eng*. 2009;32(1): 79–84.

49. Sathishkumar M, Sneha K, Yun YS. Immobilization of silver nanoparticles synthesized using *Curcuma longa* tuber powder and extract on cotton cloth for bactericidal activity. *Bioresour Technol*. 2010;101(20): 7958–7965.

50. Kalimuthu K, Babu RS, Venkataraman D, Bilal M, Gurunathan S. Biosynthesis of silver nanocrystals by *Bacillus licheniformis*. *Colloids Surf B Biointerfaces*. 2008;65(1):150–153.

51. Cullity BD, Stock SR. *Elements of X-ray Diffraction*. 3rd ed. Upper Saddle River, NJ: Prentice Hall; 2001.

52. Socrates G. *Infrared and Raman Characteristic Group Frequencies*. 3rd ed. Chichester (UK): John Wiley & Sons Ltd; 2001.

53. Teponno RB, Tapondjou AL, Djoukeng JD, et al. Isolation and NMR assignment of a pennogenin glycoside from *Dioscorea bulbifera* L. var sativa. *Nat Prod Sci*. 2006;12(1):62–66.

54. Teponno RB, Tapondjou AL, Gatsing D, et al. Bafoudiosbulbins A and B, two anti-*salmonellal* clerodane diterpenoids from *Dioscorea bulbifera* L. var sativa. *Phytochemistry*. 2006;67(17):1957–1963.

55. Teponno RB, Tapondjou AL, Abou-Mansour E, Stoeckli-Evans H, Tane P, Barboni L. Bafoudiosbulbins F and G, further clerodan editerpenoids from *Dioscorea bulbifera* L. var sativa and revised structure of bafoudiosbulbin B. *Phytochemistry*. 2008;69(12):2374–2379.

56. Wij M, Rangaswami S. Chemical constituents of *Dioscorea bulbifera* isolation and structure of a new dihydro phenanthrene 2,4,6,7, tetra-hydroxy -9,10 dihydro phenanthrene and a new phenanthrene 2,4,5,6 tetra hydroxy phenanthrene. *Indian J Chem*. 1978;16:643–644.

57. Bhandari MR, Kasai T, Kawabata J. Nutritional evaluation of wild yam (*Dioscorea* spp.) tubers of Nepal. *Food Chem*. 2003;82(4):619–623.

58. Bhandari MR, Kawabata J. Assessment of antinutritional factors and bioavailability of calcium and zinc in wild yam (*Dioscorea* spp.) tubers of Nepal. *Food Chem*. 2004;85(2):281–287.

59. Komori T. Glycosides from *Dioscorea bulbifera*. *Toxicon*. 1997;35(10):1531–1536.

60. Paknikar K. Antimicrobial activity of biologically stabilized silver nanoparticles. United States Patent US 2007/0218555A1. 2007.

61. Dibrov P, Dzioba J, Gosink KK, Hase CC. Chemiosmotic mechanism of antimicrobial activity of Ag$^+$ in *Vibrio cholera*. *Antimicrob Agents Chemother*. 2002;46(8):2668–2670.

62. Shahverdi A, Fakhimi A, Shahverdi H, Minaian S. Synthesis and effect of silver nanoparticles on the antibacterial activity of different antibiotics against *Staphylococcus aureus* and *Escherichia coli*. *Nanomedicine*. 2007;3(2):168–171.

63. Suvorova E, Klechkovskaya V, Kopeikin V, Buffat P. Stability of Ag nanoparticles dispersed in amphiphilic organic matrix. *J Cryst Growth*. 2005;275(1–2):e2351–e2356.

64. Pour NK, Dusane DH, Dhakephalkar PK, Rokhbakhsh ZF, Zinjarde SS, Chopade BA. Biofilm formation by *Acinetobacter baumannii* strains isolated from urinary tract infection and urinary catheters. *FEMS Immunol Med Microbiol*. 2011;62(3):328–338.

65. Shakibaie MR, Dhakephalkar PK, Kapadnis BP, Salayaghe G, Chopade BA. Plasmid mediated silver and antibiotic resistance in *Acinetobacter baumannii* BL54. *Iran J Med Sci*. 1998;23(12):30–36.

66. Deshpande LM, Kapadnis BP, Chopade BA. Metal resistance in *Acinetobacter* and its relation to β-lactamase production. *Bio Metals*. 1993;6(1):55–59.

67. Deshpande LM, Chopade BA. Plasmid mediated silver resistance in *Acinetobacterbaumannii* BL54. *Bio Metals*. 1994;7(1):49–56.

68. Vu H, Nikaido H. Role of beta-lactam hydrolysis in the mechanism of resistance of a beta-lactamase-constitutive *Enterobacter cloacae* strain to expanded-spectrum beta-lactams. *Antimicrob Agents Chemother*. 1985;27(3):393–398.

69. Fontana R, Amalfitano G, Rossi L, Satta G. Mechanisms of resistance to growth inhibition and killing by β-lactam antibiotics in *enterococci*. *Clin Infect Dis*. 1992;15(3):486–489.

70. Pirnay JP, De Vos D, Cochez C, et al. Molecular epidemiology of *Pseudomonas aeruginosa* colonization in a burn unit: Persistence of a multidrug-resistant clone and a silver sulfadiazine-resistant clone. *J Clin Microbiol*. 2003;41(3):1192–1202.

71. Liau SY, Read DC, Pugh WJ, Furr JR, Russell AD. Interaction of silver-nitrate with readily identifiable groups: relationship to the antibacterial action of silver ions. *Lett Appl Microbiol*. 1997;25(4):279–283.

72. Batarseh K. Anomaly and correlation of killing in the therapeutic properties of silver (I) chelation with glutamic and tartaric acids. *J Antimicrob Chemother*. 2004;54(2):546–548.